

# Origin of Ferromagnetism and its pressure and doping dependence in $Tl_2Mn_2O_7$

T. Saha-Dasgupta<sup>1</sup>, Molly De Raychaudhury<sup>1</sup> and D. D. Sarma<sup>2,\*</sup>

<sup>1</sup> *S.N. Bose National Centre for Basic Sciences, Kolkata 700098, India*

<sup>2</sup> *Solid State and Structural Chemistry Unit, Indian Institute of Science, Bangalore - 560012, India*

(Dated: February 5, 2008)

Using NMTO-*downfolding* technique, we explore and establish the origin of ferromagnetism in the pyrochlore system,  $Tl_2Mn_2O_7$ . It is found to be driven by hybridization induced spin-polarization of the delocalized charge carriers derived from Tl-*s* and O-*p* states. The mean-field estimate of the ferromagnetic transition temperature,  $T_c$ , estimated using computed exchange integrals are found to be in good agreement with the measurements. We find an enhancement of  $T_c$  for moderate doping with nonmagnetic Sb and a suppression of  $T_c$  upon application of pressure, both in agreement with experimental findings.

A range of compounds, mostly perovskites based on manganese oxide, have been found with astoundingly large negative magnetoresistance (MR). The search is on for materials with better MR properties, either in the form of colossal magnetoresistance (CMR) or tunneling magnetoresistance (TMR). Examples include systems such as double perovskites,<sup>1</sup> pyrochlores,<sup>2</sup>  $FeCr_2S_4$  and  $Fe_{0.5}Cu_{0.5}Cr_2S_4$  chalcospinels,<sup>3</sup> layered rare-earth iodide  $GdI_2$ .<sup>4</sup> While work in 1950s and 1960s uncovered<sup>5</sup> the role of double-exchange (DEX) mechanism in providing a qualitative understanding of stabilization of the ferromagnetic (FM) phase in perovskite manganites, the underlying driving mechanism for the magnetic order in diverse class of magnetoresistive materials need not be the same. Our work<sup>6</sup> on  $Sr_2FeMoO_6$  in the past has shown that driving mechanism acting in  $Sr_2FeMoO_6$  is neither the conventional double-exchange mechanism nor the super-exchange, instead a novel kinetic energy driven mechanism explains its unusual electronic and magnetic behavior. In the present communication, we focus on a pyrochlore manganite  $Tl_2Mn_2O_7$ , which has a number of contrasting properties compared to perovskite manganites. For example,  $Tl_2Mn_2O_7$  does not have mixed  $Mn^{3+}$ - $Mn^{4+}$  valences, they do not exhibit Jahn-Teller distortions in the  $MnO_6$  octahedra, and in spite of similar CMR effect observed, both the ferro- and para-magnetic phases show a metal-like behavior.

Since the discovery of CMR effect in  $Tl_2Mn_2O_7$ , it has been recognized as a class of compounds that does not fit within the DEX framework. Nevertheless, no common consensus has emerged concerning the driving mechanism in this interesting class of compounds. Considering the fact that Mn-O-Mn bond angle in  $Tl_2Mn_2O_7$  is substantially reduced<sup>7</sup> from  $180^\circ$  to  $\approx 133^\circ$ , a value that falls in the range where a sign change of the exchange interaction from antiferromagnetic to ferromagnetic is expected according to Goodenough-Kanamori rule,<sup>8</sup> a ferromagnetic superexchange picture was proposed originally.<sup>9</sup> Later on this interpretation has been questioned in view of the fact that ferromagnetic  $T_c$  is enhanced by introduction of moderate amount of nonmagnetic cation like Sb in the Mn sublattice<sup>10</sup> and gets suppressed by application of pressure,<sup>11</sup> contrary to the expectation based on super-exchange. The extended version of super-exchange idea<sup>12</sup>

has been used to explain the ferromagnetism in low  $T_c$  pyrochlore materials, making the case of  $Tl_2Mn_2O_7$  with a much larger  $T_c$  even more intriguing. Mishra and Satpathy proposed<sup>13</sup>a mechanism which is a combination of negative Hund's rule energy ( $J_H$ ) driven double exchange mechanism, antiferromagnetic super-exchange mechanism and an indirect exchange mechanism, though lacking rigorous microscopic justification for these mechanisms. In view of the enhancement of the ferromagnetic coupling in Sb substituted  $Tl_2Mn_2O_7$ , a more exotic scenario<sup>10</sup> has also been suggested with antiferromagnetic (AFM) coupling between nearest-neighbor(NN) Mn ions dominated by longer-ranged FM interactions due to the frustration of the former in the pyrochlore lattice.

Given the diversity of disparate mechanisms for ferromagnetism, we considered it worthwhile to study the underlying electronic structure model, responsible for magnetism within a rigorous and microscopic *ab-initio* theory of  $Tl_2Mn_2O_7$ . For this purpose, we have analyzed the electronic structure of  $Tl_2Mn_2O_7$ , pristine, doped with Sb and under pressure, computed within the framework of local spin density approximation (LSDA) of density functional theory (DFT) in terms of muffin-tin orbital (MTO) based NMTO-*downfolding* technique. We have also computed the magnetic exchange interaction strengths from *ab-initio* DFT calculations.

The pyrochlore structure of general stoichiometry  $A_2B_2O_6O'$  can be described as two interpenetrating networks. The smaller B cations (Mn) are octahedrally coordinated by O-type of oxygens, with the  $BO_6$  octahedra sharing corners to give rise to a  $BO_3$  network composition. The cage-like hole of this network (cf. Fig. 3) contains the second network comprising of A (Tl) and O'-type oxygens forming A-O' chains with a formula  $A_2O'$ . Self-consistent calculations were carried out within the framework of tight-binding LMTO<sup>14</sup>, for  $Tl_2Mn_2O_7$  in  $Fd\bar{3}m$  symmetry. The calculation yields a net spin moment of  $2.90 \mu_B$  per Mn atom, consistent with the measured values ( $2.74 \mu_B$  and  $2.59 \mu_B$ <sup>2,15</sup>) and the previous band-structure calculations.<sup>13,16</sup> Each Mn site with a radius of  $1.2 \text{ \AA}$  contributes  $2.57 \mu_B$ , while each  $1.0 \text{ \AA}$  O' sphere and each  $1.5 \text{ \AA}$  Tl sphere contribute  $0.24$  and  $0.08 \mu_B$ , respectively.

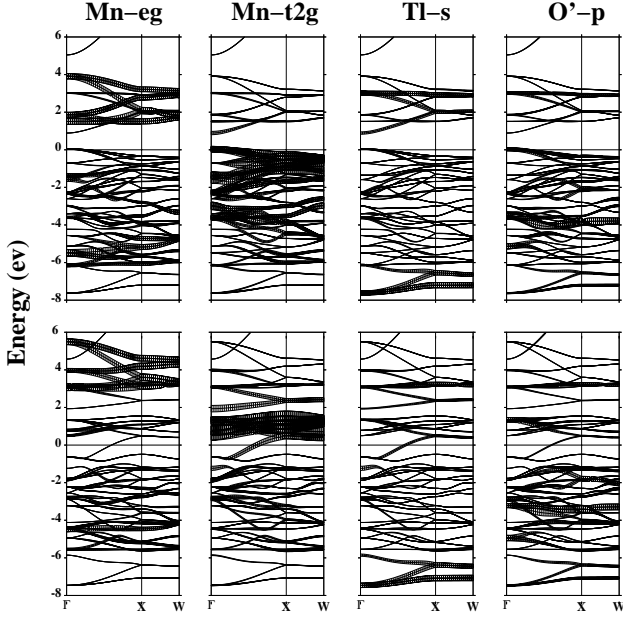


FIG. 1: Spin-polarized LDA band-structure of  $\text{Tl}_2\text{Mn}_2\text{O}_7$ . The upper panels correspond to up-spin channel and the lower panels correspond to down-spin channel. The fatness associated with the bands in each panel is proportional to the orbital character corresponding to that indicated on top of each panel.

The well-studied<sup>13,16</sup> band-structure of  $\text{Tl}_2\text{Mn}_2\text{O}_7$ , shown in Fig. 1, may be summarized as follows. The  $d-p$  hybridized band-structure extends in an energy range from about - 6 eV to 6 eV with the zero of energy set at the LSDA Fermi level,  $E_F$ . The occupied band-structure in both spin channels are dominated by  $\text{O}-p$  contributions (not shown in the figure). In the majority or up spin channel the upper part of the occupied manifold, starting from  $\approx -2$  eV is also strongly contributed by the  $\text{Mn}-t_{2g}$  states. The crystal field split  $\text{Mn}-e_g$  states span an energy range from 1.5 eV to 4 eV overlapping with the  $\text{Tl}-s - \text{O}-p$  hybrid bands. The almost full  $\text{Mn}-t_{2g}$  bands separated by a gap from  $\text{Mn}-e_g$  bands produce tiny hole pockets in the majority spin channel formed out of three almost flat bands. In the minority or down spin channel, the exchange split  $\text{Mn}-d$  bands are shifted up in energy by  $\approx 2$  eV, thereby making the  $\text{Mn}-d$  states close to empty in the down-spin channel. The noticeable feature is the highly dispersive  $\text{Mn}-t_{2g}$  band hybridized with  $\text{Tl}-s$  and  $\text{O}'-p$  that crosses  $E_F$ , producing an electron pocket in the minority spin channel. The unusually large  $\text{Tl}-\text{O}'$  hybridization produces  $\text{Tl}-\text{O}'$  bonding like states at the bottom of the spectrum at both spin channels spanning the energy from  $\approx -7$  eV to -6 eV.

The band-structure of  $\text{Tl}_2\text{Mn}_2\text{O}_7$  shows a striking similarity with that of  $\text{Sr}_2\text{FeMoO}_6$  over the low to medium energy scale. In case of  $\text{Sr}_2\text{FeMoO}_6$ ,  $\text{Fe}-d$  states are completely full in the majority spin channel, while completely empty  $\text{Mo}-d$  states appear separated from  $E_F$  by a gap of

$\approx 1$  eV. In the minority spin channel the  $t_{2g}$  manifold of the crystal field split  $\text{Fe}-d$  bands, strongly hybridized with  $\text{Mo}-t_{2g}$  (and  $\text{O}-p$ ), cross the Fermi level. These band-structure aspects suggest a strong renormalization of the spin-splitting of the  $\text{Mo}-t_{2g}$  bands (or more precisely the  $\text{Mo}-t_{2g} - \text{O}-p$  hybridized states) over its bare value, since Mo is usually *nonmagnetic* with 0.1 - 0.2 eV intrinsic exchange splitting. This was explained<sup>6</sup> in terms of the large spin splitting at the Fe site and the presence of substantial hopping between Fe and Mo sites. This situation may be directly compared with that of  $\text{Tl}_2\text{Mn}_2\text{O}_7$  with half-filled  $t_{2g}$   $3d^3$  state of Mn in  $\text{Tl}_2\text{Mn}_2\text{O}_7$  playing the role of half-filled  $3d^5$  state of Fe in  $\text{Sr}_2\text{FeMoO}_6$  and the hybridized  $\text{Tl}-\text{O}'$  state playing the role of delocalized Mo-O state in  $\text{Sr}_2\text{FeMoO}_6$ .

In the following we attempt to unravel the exchange mechanism by application of NMTO-*downfolding* technique.<sup>17</sup> NMTO-*downfolding* technique provides a useful way<sup>17</sup> to derive few-orbital Hamiltonians starting from a full LDA/LSDA Hamiltonian by integrating out degrees of freedom that are not of interest. This procedure naturally takes into account the renormalization effect due to the integrated-out orbitals by defining energy-selective, effective orbitals which serve as the Wannier or Wannier-like orbitals for the few-orbital Hamiltonian. We employ the NMTO-*downfolding* technique to construct the real-space Hamiltonian in the NMTO-Wannier function basis for  $\text{Sr}_2\text{FeMoO}_6$  and  $\text{Tl}_2\text{Mn}_2\text{O}_7$ . The O degrees of freedom for  $\text{Sr}_2\text{FeMoO}_6$  and  $\text{O}'$  degrees of freedom in case of  $\text{Tl}_2\text{Mn}_2\text{O}_7$  are downfolded to define effective Mo-O and  $\text{Tl}-\text{O}'$  states respectively. The on-site matrix elements of these real-space Hamiltonians give the estimate of various energy level positions in absence of the hybridization between the localized magnetic (Fe or Mn) and the delocalized non-magnetic (effective Mo-O or effective  $\text{Tl}-\text{O}'$ ) states. As illustrated in Fig. 2, the essentially non-magnetic Mo-O or  $\text{Tl}-\text{O}'$  states with a tiny exchange splitting ( $\leq 0.2$  eV)<sup>18</sup> appear in between the exchange split  $\text{Fe}-d$  or  $\text{Mn}-t_{2g}$  states<sup>19</sup>, respectively. On switching on the hybridization, as depicted in the right hand side of the level diagram in Fig. 2, the Mo-O or  $\text{Tl}-\text{O}'$  levels get pushed up in the up-spin channel and pushed down in the down-spin channel resulting into a large, renormalized negative spin-polarization of the mobile electron due to purely hopping interactions. The renormalized spin-splittings of the Mo-O or  $\text{Tl}-\text{O}'$  states, after switching on the hybridization, have been estimated by massive downfolding calculations. In these calculations, only the  $\text{Mo}-t_{2g}$  or  $\text{Tl}-s$  states have been kept active and all other degrees of freedom, including  $\text{Fe}-d$  or  $\text{Mn}-t_{2g}$ , have been downfolded to take into account the hybridization induced renormalization effect. Fig. 3 shows the Wannier orbitals corresponding to massively downfolded NMTO Hamiltonian in the down-spin channel for  $\text{Sr}_2\text{FeMoO}_6$  and  $\text{Tl}_2\text{Mn}_2\text{O}_7$ . The central Mo site ( $\text{Sr}_2\text{FeMoO}_6$ ) or Tl site ( $\text{Tl}_2\text{Mn}_2\text{O}_7$ ) shows the expected  $\text{Mo}-t_{2g}$  or  $\text{Tl}-s$  character, while the *tail* of the orbital sitting at the Fe and O sites ( $\text{Sr}_2\text{FeMoO}_6$ ) or Mn, O and

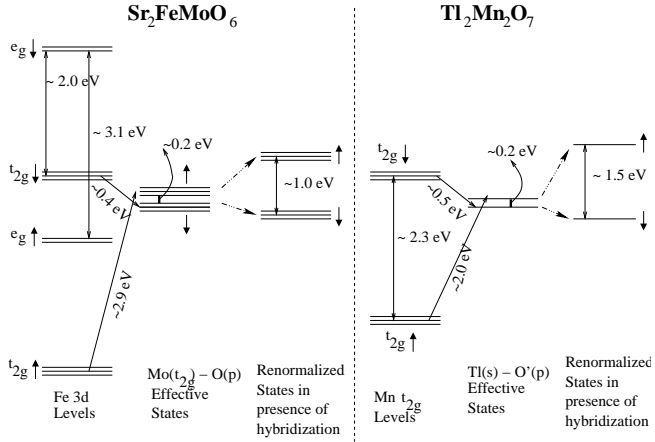


FIG. 2: Positioning of various energy levels as obtained by NMTO-*downfolding* calculation before and after switching on the hybridization between the magnetic and nonmagnetic ions.

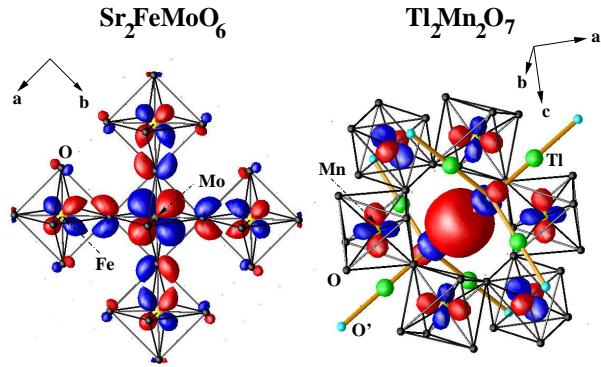


FIG. 3: (Color on-line) Effective Mo- $t_{2g}$  like and Tl-s like Wannier orbital corresponding to massively downfolded NMTO Hamiltonian in the down spin channel. Shown are the orbital shapes (constant-amplitude surfaces) with lobes of opposite signs colored as red and blue.

$O'$  sites ( $Tl_2Mn_2O_7$ ) has appreciable weight shaped according to  $Fe-t_{2g}$ ,  $O-p$  or  $Mn-t_{2g}$ ,  $O-p$ ,  $O'-p$  symmetries indicating the basic hybridization effect responsible for the renormalization. This kinetic energy driven mechanism enforces a particular spin orientation of the mobile carriers with respect of that of the localized spin, thereby providing a mechanism of ferromagnetic ordering at the localized spin sub-lattice. This is a general mechanism and will take place whenever the nonmagnetic, partially occupied level is placed within the exchange split energy levels of the magnetic ion as was emphasized in ref.20.

The above exercise demonstrates beyond any doubt that the hybridization induced negative spin-polarization mechanism similar to  $Sr_2FeMoO_6$  to be operative also in case of  $Tl_2Mn_2O_7$ . The reason that in case of  $Tl_2Mn_2O_7$ , Tl in contrast exhibits a net *positive* moment as opposed to the ferrimagnetic spin alignment of Fe and Mo states in  $Sr_2FeMoO_6$ , is the unusual covalency of Tl-O' and

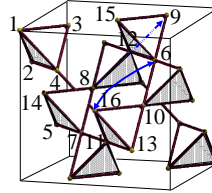


TABLE I: Magnetic configurations of the Mn ions in the supercell for the states used to determine the magnetic interactions. The numbering of the Mn ions are as shown in the picture. The last column gives the relative LSDA energies per Mn ion in meV.

	1	2	3	4	5	6	7	8	9	10	11	12	13	14	15	16	$\Delta E$
FM	+	+	+	+	+	+	+	+	+	+	+	+	+	+	+	+	0
AFM1	+	-	+	+	+	-	+	+	+	-	+	+	-	+	+	+	9.55
AFM2	-	-	-	+	-	+	+	-	-	-	-	+	-	-	-	-	13.98
AFM3	+	+	-	-	+	-	-	+	+	-	-	+	+	-	-	-	12.24
AFM4	-	-	+	+	-	+	+	+	+	-	-	+	-	-	-	-	17.59
AFM5	-	-	+	+	-	-	+	+	-	+	-	+	-	-	-	-	18.39

mixing with Mn-O states which extends till the bottom of the spectra.<sup>16</sup>

We now turn to estimate quantitatively the exchange interaction strengths, and therefore  $T_c$ . We compute the exchange integrals by comparing the LSDA total energies of different spin configurations to that of an effective Heisenberg Hamiltonian constructed out of  $Mn^{4+}$  spins. The network of Mn ions in  $Tl_2Mn_2O_7$ , as shown in Table I, is an infinite three-dimensional lattice of corner-sharing tetrahedra. Such a geometrical arrangement gives rise to a very high degree of frustration for AFM, NN interactions. Due to this frustration, it is not possible to satisfy the antiferromagnetism completely, and the chosen AFM configurations invariably have net magnetic moments. The energy differences of all the AFM configurations relative to FM configuration are positive, implying FM state as the stable ground state consistent with experimental findings.

The effective Heisenberg Hamiltonian, considering till 3NN interactions (six NN, twelve second NN and twelve third NN), can be written as,

$$H = J_1 \sum_{nn} S_i \cdot S_j + J_2 \sum_{2nn} S_i \cdot S_j + J_3 \sum_{3nn} S_i \cdot S_j \quad (1)$$

where  $S_i$  denotes the spin-3/2 operator corresponding  $Mn^{4+}$  states at site  $i$ , and  $J_1$ ,  $J_2$ ,  $J_3$  denote the NN, 2NN and 3NN magnetic exchange interaction strengths. For the calculation of exchange couplings, the computed LSDA energies were fitted to the mean-field Heisenberg model, which contains Ising terms of the full Hamiltonian (1). A well-known limitation of this approach is that in some cases the result depends on the choice of spin configurations. To overcome this we obtained seven different estimates of  $J_1$ ,  $J_2$  and  $J_3$  employing various independent combinations of five different energies listed in Table I. Our calculation gives the average estimate of  $J_1$ ,  $J_2$ ,  $J_3$  as -2.52 meV, -0.11 meV and 0.33 meV with a standard deviation of 0.24 meV, 0.06 meV and 0.08 meV, respectively. Substituting the estimated values of  $J_1$ ,  $J_2$ ,  $J_3$  in the mean-field estimate of  $T_c$ :  $T_c^{mf} = \frac{S(S+1)J_o}{3k_B}$ , where

$J_o$ , the net effective interaction is  $6J_1 + 12J_2 + 12J_3$ ,  $S=3/2$  and  $k_B$  is the Boltzmann constant, gives a  $T_c$  of 181 K. This is a very reasonable estimate considering mean-field overestimation and experimentally measured value of 142 K.<sup>2</sup>

As mentioned in the beginning, magnetic properties of  $Tl_2Mn_2O_7$  exhibit interesting variations with Sb-substitution and under pressure. We have addressed these issues within the present approach. We mention here only the salient points of our study, the details of the calculation will be reported elsewhere.<sup>22</sup> To mimic the Sb-substitution, we have carried out calculations with eight formula unit supercells, where 1 and 2 out of 16 Mn atoms are replaced by Sb, corresponding to a doping level of 6.25 % and 12.5 %, respectively. Due to the slightly larger size of Sb, lattice parameters and bond lengths increase by less than 1% with no appreciable change in bond angles.<sup>10</sup> The computed electronic structure shows the overall band shapes to remain more or less same with electron doping in the strongly hybridized  $Tl-s-O-p-Mn-t_{2g}$  conduction band in the down spin channel. This causes a substantial rise in the density of states of the conduction band at  $E_F$ , from 0.2 eV<sup>-1</sup> for the undoped case to 1.0 eV<sup>-1</sup> and 1.4 eV<sup>-1</sup> for 6.25 % and 12.5 % doped cases, respectively. Within the framework of the proposed mechanism, this is expected to lead to a strong enhancement of the magnetic coupling.<sup>21</sup> This is supported by our computed  $J$ 's from LSDA total energy calculations, which necessarily includes the proposed kinetic energy driven exchange. The mean field estimate of  $T_c$  is found to be 382 K and 420 K for 6.25 % and 12.5 % doping concentrations, respectively. Though the trend is in agreement with the experimental observations,<sup>10</sup> the enhancement is grossly overestimated, presumably due to clustering and disordering effects, not taken into account in the calculation.

Existing proposals for structural changes under pressure are controversial. The first paper<sup>11</sup> reported a decrease of Mn-O-Mn bond angle, in addition to a decrease of bond lengths. Subsequent measurements<sup>23</sup> claim the Mn-O-Mn bond angle to increase. In absence of a clear consensus about the structural changes, we carried out two sets of calculations. In the first set, the pressure applied is assumed to be isotropic, so that only the bond

lengths are assumed to decrease. In the second set, we also changed the Mn-O-Mn bond angle, taken according to Fig. 2 of ref.23. Using the first set of calculations, the mean field estimate of  $T_c$  derived from our computed  $J$ 's, show a decrease of  $T_c$  by 40 K upon 2 % change in bond lengths. In second set of calculations, where we also changed the Mn-O-Mn bond angle, which according to ref<sup>23</sup> for 2% decrease in bond length, increases by less than 1°, the  $T_c$  is found to decrease further by 7 K<sup>24</sup>. From analysis of electronic structure, upon application of pressure, the bond lengths shorten which in turn enhances the Mn-O and Tl-O' interactions resulting into the broadening of the net band width. The more important effect for the present issue, however, is that the delocalized Tl-O' effective levels are found to shift<sup>25</sup>. As is evident from the level diagram in Fig. 2, the strength of the hybridization between the magnetic and the non-magnetic states depends crucially on the positioning of the various energy levels. The movement of the energy levels causes changes in hybridization strengths, leading to suppression in the kinetically driven magnetic interactions and hence in a reduction of  $T_c$ . The small increase of Mn-O-Mn bond angle in the second set of calculations, which is a secondary effect on top of the former effect, increases the antiferromagnetic super-exchange contribution resulting into further suppression of ferromagnetic  $T_c$ .

To conclude, we have shown by means of NMTO based *downfolding* study that the underlying mechanism of ferromagnetism in  $Tl_2Mn_2O_7$  is a kinetic energy driven mechanism originally proposed for  $Sr_2FeMoO_6$ . The mean field  $T_c$ , estimated using computed  $J$ 's is in good agreement with experiments. For  $Tl_2Mn_2O_7$  moderately doped with Sb, we found an enhancement in  $T_c$  and on application of pressure,  $T_c$  is found to decrease, both in agreement with experimental observations. The microscopic origin of these changes in  $T_c$  are found to be dominantly due to changes in the magnetic interaction strengths arising from the proposed kinetically-driven mechanism.

The research was funded by DST project SR/S2/CMP-42/2003. We thank MPG-partnergroup program for the collaboration.

\* Also at Jawaharlal Nehru Center for Advanced Scientific Research and Center for Condensed Matter Theory, IISc.

<sup>1</sup> K. I. Kobayashi *et. al.*, Nature(London), **395**, 677 (1998).

<sup>2</sup> Y. Shimakawa *et. al.*, Nature(London), **379**, 53 (1996).

<sup>3</sup> A. Ramirez *et. al.*, Nature(London), **386**, 156 (1997).

<sup>4</sup> C. Felser *et. al.* J. Solid State Chem **147** 19 (1999).

<sup>5</sup> P. W. Anderson and H. Hasegawa, Phys. Rev. **100** 675 (1955); P.-G. DeGennes, Phys. Rev. **118** 141 1960).

<sup>6</sup> D. D. Sarma *et. al.*, Phys. Rev. Lett **85**, 2549 (2000).

<sup>7</sup> A. Ramirez and M. Subramanian, Science **277**, 546 (1997).

<sup>8</sup> J. B. Goodenough, Phys. Rev. **100** 564 (1995).

<sup>9</sup> Y. Shimakawa *et. al.*, Phys. Rev. B **55** 6399 (1997).

<sup>10</sup> J. A. Alonso *et. al.*, Phys. Rev. B **60** R 15024 (1999).

<sup>11</sup> Yu. V. Sushko *et. al.*, Physica B **259-261** 831 (1999).

<sup>12</sup> M. D. Núñez-Regueiro and G. Lacroix, Phys. Rev. B **63** 014417 (2000).

<sup>13</sup> S. K. Mishra and S. Satpathy, Phys. Rev. B **58** 7585 (1998).

<sup>14</sup> O. K. Andersen and O. Jepsen, Phys. Rev. Lett. **53** 2571 (1984).

<sup>15</sup> M. A. Subramanian *et. al.* Science **273**, 81 (1996).

<sup>16</sup> D. J. Singh, Phys. Rev. B **55** 313 (1997).

<sup>17</sup> O. K. Andersen and T. Saha-Dasgupta, Phys. Rev. B **62**

R16219 (2000); See references in O. K. Andersen *et. al.*, Bull. Mater. Sci **26** 19 (2003).

<sup>18</sup> The tiny splitting comes from the electrostatic effect.

<sup>19</sup> Empty Mn- $e_g$  does not contribute in the mechanism.

<sup>20</sup> D. D. Sarma, Current Opinion in Solid State & Materials Science, **1** (2001)

<sup>21</sup> J. Kanamori and K. Terakura, J. Phys. Soc. Jpn. **70**, 1433 (2001).

<sup>22</sup> M. De Raychaudhury *et. al.*, unpublished.

<sup>23</sup> P. Velasco *et. al.*, Phys. Rev. B **67** 104403 (2003).

<sup>24</sup> Considering the experimental estimate of the pressure corresponding to 2% bond length change and accounting for the mean field overestimation, the two sets of calculations lead to  $dT_c/dP$  as -2.7 K/GPa and -3.2 K/GPa respec-

tively, which overestimates the experimental estimate of  $\approx$  -1.6 – -1 K/GPa. However, it is necessary to clarify the experimental scenario in terms of precise structural determination. If Mn-O-Mn bond angle indeed decreases as was suggested in the first paper, then the theoretical estimate of  $dT_c/dP$  will be closer to experimental value.

<sup>25</sup> The energy level positions obtained by NMTO-downfolding technique show a shift of Tl-O' derived states relative to Mn- $t_{2g}$  by +0.3 eV on applying the pressure. This energy shift more than compensates for the slight increase in the hopping interaction due to the 0.07 Å compression in Mn-Tl bond length.